Monthly Notices of the ROYAL ASTRONOMICAL SOCIETY

MNRAS **515,** 6066–6072 (2022) https://doi.org/10.1093/mnras/stac2109
Advance Access publication 2022 July 29

A quantum mechanical calculation of the CN radiative association

Shuai Zhang,[1] Zhi Qin [1,2]★ and Linhua Liu [1,2,3]★

[1]*School of Energy and Power Engineering, Shandong University, Jinan, Shandong 250061, China*
[2]*Optics & Thermal Radiation Research Center, Institude of Frontier and Interdisciplinary Science, Shandong University, Qingdao, Shandong 266237, China*
[3]*School of Energy Science and Engineering, Harbin Institute of Technology, Harbin 150001, China*

Accepted 2022 July 24. Received 2022 July 23; in original form 2022 April 8

ABSTRACT

Radiative association of CN is investigated through the quantum mechanical method, including the cross sections and rate coefficients. The *ab initio* potential energy curves, transition dipole moments, and permanent dipole moments of CN are obtained by the internally contracted multireference configuration interaction method with Davidson correction and aug-cc-pwCV5Z-DK basis set. For the collision of the ground state C (^3P_g) and N (^4S_u) atoms, except for the four previously studied processes including the $A^2\Pi \rightarrow X^2\Sigma^+$, $X^2\Sigma^+ \rightarrow A^2\Pi$, $A^2\Pi \rightarrow A^2\Pi$, and $X^2\Sigma^+ \rightarrow X^2\Sigma^+$ transitions, four other radiative association processes including $b^4\Pi \rightarrow a^4\Sigma^+$, $a^4\Sigma^+ \rightarrow b^4\Pi$, $b^4\Pi \rightarrow b^4\Pi$, and $a^4\Sigma^+ \rightarrow a^4\Sigma^+$ transitions are considered. We also considered the collision of the excited C (^1D_g) and the ground N (^4S_u) atoms including the $2^4\Pi \rightarrow 1^4\Sigma^-$ process and the collision of the ground C (^3P_g) and the excited N (^2D_u) atoms including $2^2\Pi \rightarrow B^2\Sigma^+$, $3^2\Pi \rightarrow B^2\Sigma^+$, and $4^2\Pi \rightarrow B^2\Sigma^+$ transitions. The temperature population factor is considered to describe the thermal population of the three different dissociation asymptotic energies. The results show that the contribution of the $A^2\Pi \rightarrow X^2\Sigma^+$ and $b^4\Pi \rightarrow a^4\Sigma^+$ transitions to the total rate coefficients is significant over the entire temperature range. While considering the collision of C and N involving excited states, the contribution of the $2^2\Pi \rightarrow B^2\Sigma^+$, $3^2\Pi \rightarrow B^2\Sigma^+$, and $4^2\Pi \rightarrow B^2\Sigma^+$ transitions to the total rate coefficients cannot be ignored at the temperature range larger than 10 000 K. Finally, the rate coefficients are fitted to an analytical function for astrochemical reaction modelling.

Key words: astrochemistry – molecular data – molecular processes.

1 INTRODUCTION

Radiative association means that two free fragments form a stable molecule through collision with photon emission and is one important way for the formation of small molecules in the interstellar medium (Klemperer 1971). Only for certain ionic systems, the direct laboratory measurements of their radiative association can be possible to carry out (Gerlich & Horning 1992). Therefore, to study the chemical evolution in the interstellar space, various theoretical methods, such as the classical method, semiclassical (SC) method, and quantum mechanical (QM) method (Nyman, Gustafsson & Antipov 2015), have been developed. These methods have been extensively used to study small molecules in astrophysical environments especially for diatomic molecules such as CO (Dalgarno, Du & You 1990), N_2 (Smith 1993), N_2^+ (Qin, Bai & Liu 2021), SiN (Singh et al. 1999; Gustafsson & Forrey 2019), MgO (Bai, Qin & Liu 2021), BeH^+ (Szabó, Góger & Gustafsson 2021), AlO (Bai, Qin & Liu 2022), and etc.

CN is a radical of great astrophysical importance and it has been observed in sun (Lambert 1968; Sneden & Lambert 1982), stellar atmospheres (Wootten et al. 1982; Lambert et al. 1984; Bachiller et al. 1997), diffuse interstellar clouds (Morton 1975; Meyer & Jura 1985; Black & van Dishoeck 1988; Lambert, Sheffer & Crane 1990; Crawford 1995), and dense clouds (Turner & Gammon 1975; Gerin et al. 1984; Greaves & Church 1996). The CN radical is also discovered in late-type red giant stars as an indication of the atomic nitrogen abundance (Duric, Erman & Larsson 1978; Lambert 1978) and can provide information about the photochemical history of cometary molecules (Combi 1980; Johnson, Fink & Larsson 1983). As for the CN radiative association, the researches through the classical method (Singh & Andreazza 2000; Gustafsson 2013), SC method (Gustafsson & Forrey 2019), and QM method (Antipov et al. 2009) have been carried out. However, these studies only focus on the $A^2\Pi \rightarrow X^2\Sigma^+$, $X^2\Sigma^+ \rightarrow A^2\Pi$, $A^2\Pi \rightarrow A^2\Pi$, and $X^2\Sigma^+ \rightarrow X^2\Sigma^+$ transition processes.

The studies about N_2^+ (Qin et al. 2021) and AlO (Bai et al. 2022) show that radiative association through high excited electronic states of the formed molecule may impact the total rate coefficients for the colliding ground-state atoms. Also, the exploration about the radiative association of MgO (Bai et al. 2021) shows the possible importance for the colliding atoms in their excited states. Balucani et al. (2010) studied the formation of nitriles and imines on the reaction dynamics of excited N (^2D_u) atoms with ethane in the atmosphere of Titan. Feldman & Brune (1976) had found that a substantial amount of resonance scattering from metastable C (^1D_g) atoms at the ionospheres of the comets Kahoutek and West. These researches show that the formation of the molecule in its high-lying electronic states through the collision of ground or excited-state atoms may make sense in particular cases. Therefore, besides

★ E-mail: z.qin@sdu.edu.cn (ZQ); liulinhua@sdu.edu.cn (LL)

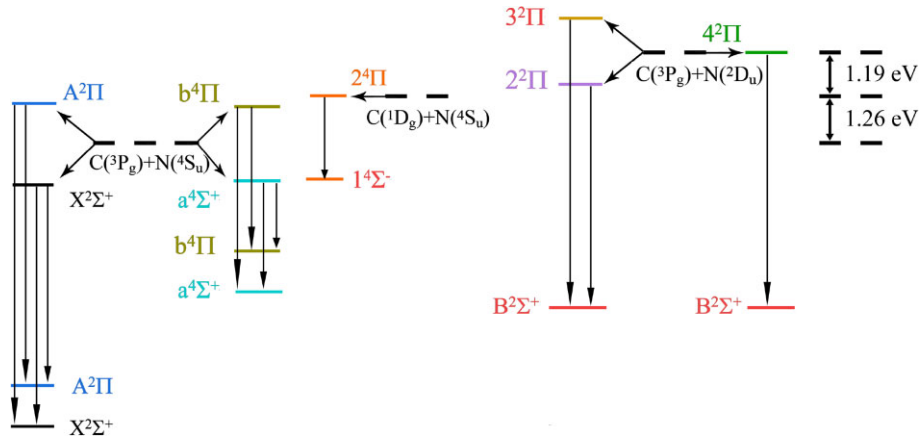

Figure 1. An overview of twelve radiative association transitions including the 10 electronic states of the CN radical corresponding to the dissociation limits of C (^3P_g) + N (^4S_u), C (^1D_g) + N (^4S_u), and C (^3P_g) + N (^2D_u).

the four transition processes of CN mentioned before, this work also considers the other four radiative association processes for the ground C (^3P_g) and N (^4S_u) atoms, one radiative association process for the collision of the excited C (^1D_g) and the ground N (^4S_u) atoms, and three radiative association processes for the collision of the ground C (^3P_g) and the excited N (^2D_u) atoms. An overview of all considered radiation association processes is shown in Fig. 1, specifically including the following reactions:

$$A^2\Pi\left[C\left(^3P_g\right)+N\left(^4S_u\right)\right]\rightarrow CN\left(A^2\Pi\right)+h\nu \quad (1)$$

$$A^2\Pi\left[C\left(^3P_g\right)+N\left(^4S_u\right)\right]\rightarrow CN\left(X^2\Sigma^+\right)+h\nu \quad (2)$$

$$X^2\Sigma^+\left[C\left(^3P_g\right)+N\left(^4S_u\right)\right]\rightarrow CN\left(X^2\Sigma^+\right)+h\nu \quad (3)$$

$$X^2\Sigma^+\left[C\left(^3P_g\right)+N\left(^4S_u\right)\right]\rightarrow CN\left(A^2\Pi\right)+h\nu \quad (4)$$

$$b^4\Pi\left[C\left(^3P_g\right)+N\left(^4S_u\right)\right]\rightarrow CN\left(b^4\Pi\right)+h\nu \quad (5)$$

$$a^4\Sigma^+\left[C\left(^3P_g\right)+N\left(^4S_u\right)\right]\rightarrow CN\left(a^4\Sigma^+\right)+h\nu \quad (6)$$

$$b^4\Pi\left[C^3P_g\right)+N\left(^4S_u\right)\right]\rightarrow CN\left(a^4\Sigma^+\right)+h\nu \quad (7)$$

$$a^4\Sigma^+\left[C\left(^3P_g\right)+N\left(^4S_u\right)\right]\rightarrow CN\left(b^4\Pi\right)+h\nu \quad (8)$$

$$2^4\Pi\left[C\left(^1D_g\right)+N\left(^4S_u\right)\right]\rightarrow CN\left(1^4\Sigma^-\right)+h\nu \quad (9)$$

$$2^2\Pi\left[C\left(^3P_g\right)+N\left(^2D_u\right)\right]\rightarrow CN\left(B^2\Sigma^+\right)+h\nu \quad (10)$$

$$3^2\Pi\left[C\left(^3P_g\right)+N\left(^2D_u\right)\right]\rightarrow CN\left(B^2\Sigma^+\right)+h\nu \quad (11)$$

$$4^2\Pi\left[C\left(^3P_g\right)+N\left(^2D_u\right)\right]\rightarrow CN\left(B^2\Sigma^+\right)+h\nu \quad (12)$$

The cross sections and rate coefficients for the formation of the CN molecule through the reaction (1) to reaction (12) are calculated. The results show that taking more radiative association processes related to high excited states into account improves the CN rate coefficients.

This work is organized as follows, the theory and methods for calculating the CN electronic structure and radiative association are given in Section 2. The results and discussion of the potential energy curves (PECs), transition dipole moments (TDMs), permanent dipole moments (PDMs), radiative association cross sections, and rate coefficients are presented in Section 3. The conclusion is drawn in Section 4.

2 THEORY AND METHODS

2.1 Potential energy and dipole moment curves

In order to study radiative association processes of the CN molecule, the PECs of the 11 electronic states including the $X^2\Sigma^+$, $A^2\Pi$, $a^4\Sigma^+$, $b^4\Pi$, $1^4\Sigma^-$, $2^4\Pi$, $1^4\Delta$, $B^2\Sigma^+$, $2^2\Pi$, $3^2\Pi$, and $4^2\Pi$ states, TDMs of the $A^2\Pi$–$X^2\Sigma^+$, $2^2\Pi$–$B^2\Sigma^+$, $3^2\Pi$–$B^2\Sigma^+$, $4^2\Pi$–$B^2\Sigma^+$, $b^4\Pi$–$a^4\Sigma^+$, $2^4\Pi$–$1^4\Sigma^-$, and $2^4\Pi$–$1^4\Delta$ transitions, and PDMs of the $X^2\Sigma^+$, $A^2\Pi$, $a^4\Sigma^+$, and $b^4\Pi$ states were calculated with the MOLPRO 2015 quantum chemistry package (Werner et al. 2015, 2020). MOLPRO cannot deal with the symmetry of the non-Abelian so that we replaced the $C_{\infty v}$ symmetry of the CN molecule with C_{2v} symmetry. The irreducible representation of the C_{2v} point group is (a_1, b_1, b_2, a_2) and its corresponding relationship to $C_{\infty v}$ point group can be described as follows: $\Sigma^+ \rightarrow a_1$, $\Sigma^- \rightarrow a_2$, $\Pi \rightarrow (b_1, b_2)$, $\Delta \rightarrow (a_1, a_2)$. The computation is divided into three steps. First, the Hartree-Fock (HF) self-consistent field method was used to calculate the molecule orbits (MOs) and potential energy of the ground state. Secondly, to generate multiconfiguration wavefunctions for 11 electronic states, the state-averaged complete active space self-consistent field calculations (Werner & Knowles 1985; Knowles & Werner 1985) were carried out based on the HF MOs. Finally, the internally contracted multireference configuration interaction method including Davidson correction (icMRCI+Q) (Werner & Knowles 1988; Knowles & Werner 1992, 1988; Shamasundar, Knizia & Werner 2011) was used to consider the dynamic correlation and size-consistency error. The aug-cc-pwCV5Z-DK Gaussian basis was selected to consider the effects of core-valence correlation and scalar relativistic effects.

The judiciously chosen active space furnishes smooth and reliable PECs, TDMs and PDMs especially for those in high-lying electronic states. The electronic shell structures of the C and N atom are $1s^22s^22p^2$ and $1s^22s^22p^3$, respectively. Both of their inner orbits are described by $1s$ which was chosen to be closed as reference space corresponding to the MOs (2, 0, 0, 0). The valence MOs (4, 2, 2, 0) and the virtual orbits (2, 1, 1, 0) are chosen as the active space. For high-lying Π electronic states (namely $2^2\Pi$, $3^2\Pi$, $4^2\Pi$), the virtual obits (1, 2, 2, 0) are selected for better relaxation of the wavefunctions and the smooth computation for the whole internuclear distances considered here. Finally, in the calculation of PECs and TDMs for CN, 88 points are considered for the internuclear distances of 0.8–10

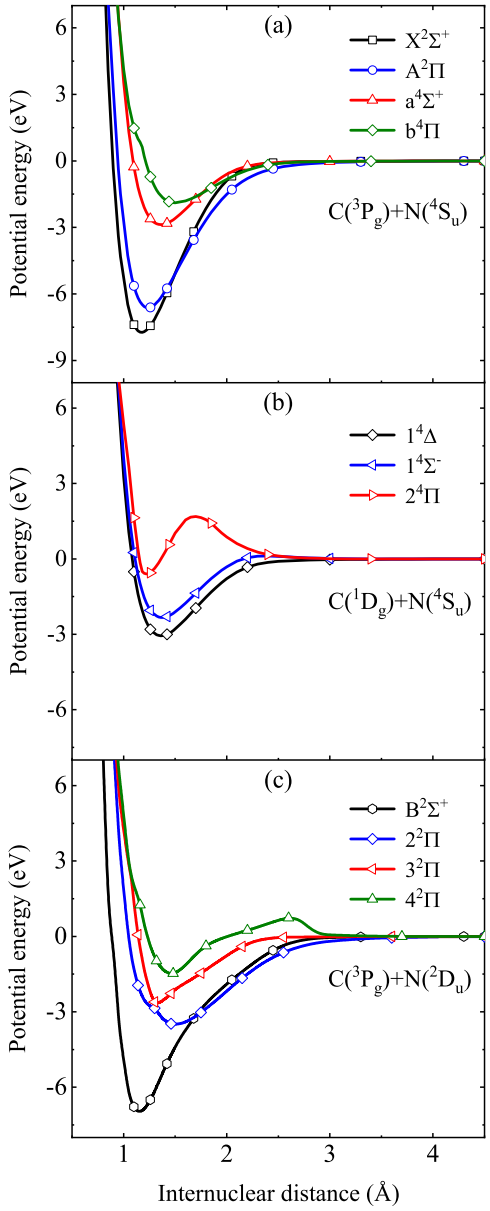

Figure 2. PECs of the electronic states for CN calculated by the icMRCI+Q/aug-cc-pwCV5Z-DK method corresponding to the dissociation limits of (a) C (^3P_g) + N (^4S_u), (b) C (^1D_g) + N (^4S_u), and (c) C (^3P_g) + N (^2D_u). The symbols on the PECs are data points displayed by skipping eight points.

Å with step sizes of 0.05 Å for 0.8–1 Å, 0.02 Å for 1–2 Å, 0.05 Å for 2–3 Å, 0.5 Å for 3–10 Å.

For internuclear distances R larger than 10 Å until to 50 Å, the following function was used to fit the PECs, TDMs, and PDMs

$$V(R) = -\frac{C_5}{R^5} - \frac{C_6}{R^6} + V(R \to \infty), \tag{13}$$

where C_5 represents the fitting coefficient. The values C_5 is estimated by fitting *ab initio* points while keeping the dissociation limits and C_6 fixed. C_6 is the dipole–dipole coefficient which was obtained by the London formula (Magnasco, Ficari & Battezzati 1977)

$$C_6 = \frac{3}{2}\frac{\Gamma_C \Gamma_N}{\Gamma_C + \Gamma_N}\alpha_C \alpha_N, \tag{14}$$

where Γ is the ionization energy of the atom, which are obtained from NIST Atomic Spectra Database (Kramida et al. 2021). α is the static dipole polarizability. For R smaller than 0.8 Å, the PECs were extrapolated to zero by the following function:

$$V(R) = A\exp(-BR) + C, \tag{15}$$

where A, B, and C are fitting parameters. The TDMs and PDMs were also extrapolated to zero by using equation (15). To ensure a continuous and smooth PEC, the cubic spline was used to interpolate the *ab initio* points.

2.2 Radiative association cross sections

The quantum mechanical expression of the radiative association cross section is as follows:

$$\sigma_{\Lambda'\to\Lambda''} = \sum_{J'',V'',J''} \frac{1}{4\pi\varepsilon_0}\frac{64}{3}\frac{\pi^5}{k^2} g_{\Lambda'} \left(\frac{\omega}{c}\right)^3 S_{\Lambda',J'\to\Lambda'',J''} \times \left|M_{\Lambda',E,J';\Lambda'',v'',J''}\right|^2 \tag{16}$$

where the symbol of single prime '′' means the physical quantity of the initial electronic state, while the double prime '″' represents the physical quantity of the final electronic state. Λ describes the absolute value of the projection of the electronic orbital angular momentum on the internuclear axis, ε_0 denotes the vacuum permittivity, $k^2 = 2E\mu/\hbar^2$, ω is the frequency of the emitted photon, c is the speed of light in vacuum and $S_{\Lambda',J'\to\Lambda'',J''}$ represents the Hönl-London factor (Hansson & Watson 2005; Watson 2008). The $g_{\Lambda'}$ is the probability of collision for the initial electronic state Λ', given by

$$g_{\Lambda'} = \frac{(2S+1)\left(2-\delta_{0,\Lambda}\right)}{(2L_C+1)(2S_C+1)(2L_N+1)(2S_N+1)}, \tag{17}$$

where δ is the Kronecker delta. S is the spin quantum number of the electronic state Λ'. L and S are the electronic orbital angular momentum number and spin quantum number, respectively. The subscripts C and N represent the C and N atoms, respectively. Therefore, the values of $g_{\Lambda'}$ are 2/36 for $X^2\Sigma^+$, 4/36 for $A^2\Pi$ and $a^4\Sigma^+$, 8/36 for $b^4\Pi$, 8/20 for $2^4\Pi$, and 4/90 for $2^2\Pi$, $3^2\Pi$, $4^2\Pi$. $M_{\Lambda',E,J';\Lambda'',v'',J''}$ is the electronic transition moment function, given by

$$M_{\Lambda',E,J';\Lambda'',v'',J^n} = \left\langle \chi_{E,J'}(R)|D(R)|\psi_{v'',J''}(R)\right\rangle, \tag{18}$$

where $D(R)$ is the TDM. $\chi_{E,J'}(R)$ is the radial wavefunction of an initial continuum state, $\psi_{v'',J''}(R)$ is the radial wavefunction of a rovibrational bound state. The continuum and bound wavefunctions are obtained by using the renormalized Numerov method (Johnson 1977, 1978).

2.3 Rate coefficients

The total rate coefficients $\alpha_{\rm tot}(T)$ of forming a bound molecule can be expressed as

$$\alpha_{\rm tot}(T) = \sum_{\Lambda'\to\Lambda''} \alpha_{\Lambda'\to\Lambda''}(T), \tag{19}$$

where $\alpha_{\Lambda'\to\Lambda''}(T)$ represents the thermal rate coefficients for an electronic transition process $\Lambda' \to \Lambda''$, $\alpha_{\Lambda'\to\Lambda''}$ can be calculated as a function of temperature T:

$$\alpha_{\Lambda'\to\Lambda''}(T) = \sqrt{\frac{8}{\pi\mu\left(k_{\rm B}T\right)^3}}\int_0^\infty E\sigma_{\Lambda'\to\Lambda''}(E)\mathrm{e}^{(-E/k_{\rm B}T)}\mathrm{d}E, \tag{20}$$

Table 1. Spectroscopic constants for electronic states of CN.

State	Method	R_e (Å)	D_e (eV)	ω_e (cm^{-1})	$\omega_e\chi_e$ (cm^{-1})	B_e (cm^{-1})	α_e (cm^{-1})
$X^2\Sigma^+$	Calc.[a]	1.1749	7.7432	2057.426	13.841	1.887	0.0165
	Expt.[b]	1.1718	–	2068.68	13.122	1.8998	0.01737
	Expt.[c]	1.1718	–	2068.65	13.079	1.8998	0.01737
	Expt.[d]	1.1718	–	2068.59	13.087	1.8997	0.01736
	Calc.[e]	1.1759	7.7072	2056.9	13	1.886	0.0172
	Calc.[f]	1.1714	7.8206	2069.26	10.231	1.9013	0.01719
	Calc.[g]	1.175	7.74	2062.3	13.11	1.89	–
$B^2\Sigma^+$	Calc.[a]	1.1549	6.9757	2154.52	22.71	1.964	0.0215
	Expt.[c]	1.1511	–	2160.38	17.744	1.9688	0.01996
	Expt.[d]	1.15	–	2163.9	20.2	1.973	0.023
	Calc.[i]	1.1508	–	2164.83	17.686	1.9699	0.02007
	Calc.[e]	1.1549	6.9255	2161.3	21.93	1.959	0.021
	Calc.[f]	1.151	7.025	2163.04	14.789	1.9554	0.01908
$A^2\Pi$	Calc.[a]	1.2365	6.6337	1798.956	12.653	1.706	0.01704
	Expt.[c]	1.2331	–	1813.24	12.751	1.7156	0.01712
	Expt.[d]	1.2333	–	1812.56	12.609	1.7151	0.01708
	Calc.[f]	1.2324	6.6912	1814.75	13.053	1.7174	0.01708
	Calc.[i]	1.2332	–	1811.47	12.601	1.715	0.01721
	Calc.[g]	1.238	6.61	1809.0	12.77	1.70	–
$2^2\Pi$	Calc.[a]	1.5033	3.5033	1031.769	18.606	1.1563	0.0185
	Calc.[h]	1.466	–	1207	19	1.214	–
$4^2\Pi$	Calc.[a]	1.4657	2.3781	1376.312	14.449	1.214	0.0019
	Calc.[h]	1.448	–	1359	16.9	1.244	–
$a^4\Sigma^+$	Calc.[a]	1.3611	2.9143	1300.875	8.648	1.407	0.0176
	Calc.[i]	1.3629	–	1315.67	12.623	1.4091	0.0315
$3^2\Pi$	Calc.[a]	1.3233	2.667	2158.966	160.645	1.487	0.0666
$b^4\Pi$	Calc.[a]	1.5021	1.9171	973.679	12.362	1.151	0.0175
	Calc.[f]	1.502	1.8841	982.48	11.325	1.15363	0.0177
$2^4\Pi$	Calc.[a]	1.2257	2.3018	2107.743	9.302	1.715	0.0335
	Calc.[f]	1.2201	2.3626	2578.69	300.34	1.7503	0.08259
$1^4\Sigma^-$	Calc.[a]	1.3695	2.4935	1237.029	11.062	1.388	0.0204
	Calc.[f]	1.3674	2.34	1266.48	13.262	1.39517	0.01942

Note. [a]This work, [b]Ram et al. (2006), [c]Prasad & Bernath (1992), [d]Huber & Herzberg (1979), [e]Rosati et al. (2007), [f] Yin et al. (2018), [g]Antipov et al. (2011), [h]Lavendy, Robbe & Gandara (1987), [i]Shi et al. (2011).

where μ is the reduced mass, k_B is the Boltzmann constant, E is the collision energy, and $\sigma_{\Lambda'\to\Lambda''}$ is the cross section of the $\Lambda' \to \Lambda''$ electronic transition.

3 RESULTS AND DISCUSSION

3.1 PECs and TDMs

Based on the approaches described in Section 2.1, the PECs of 11 electronic states for CN are calculated at the icMRCI+Q/aug-cc-pwCV5Z-DK level of theory and are shown in Fig. 2. The values of PECs dissociating to the corresponding asymptote are defined as the potential energy zero-points of different electronic states, respectively. To ensure the accuracy of PECs, the fitted spectroscopic constants are listed in Table 1, along with the results of previous theoretical calculations and experiments. The calculated spectroscopic constants are in good agreement with those determined by experiments (Huber & Herzberg 1979; Prasad & Bernath 1992; Ram et al. 2006). The R_e and ω_e values differ by a maximum of 0.038 Å and 14.284 cm^{-1}, respectively. The PECs for the $1^4\Delta$ and $1^4\Sigma^-$ states are extremely similar because the electronic configurations of both states have nearly the same weight. The avoided crossing occurs between the $2^2\Pi$ and $3^2\Pi$ states near 1.3 Å due to the adiabatic approximation assumption. For other high-lying excited states, the spectroscopic constants are compared with the available theoretical ones (Lavendy, Robbe & Gandara 1987; Shi et al. 2011; Yin et al. 2018) and they are in good agreement.

The radiation association cross sections depend on the square of the dipole moments and the third power of the electronic transition energies. Therefore, the transitions with small values of TDMs, such as the $2^2\Pi$–$X^2\Sigma^+$, $3^2\Pi$–$X^2\Sigma^+$, and $4^2\Pi$–$X^2\Sigma^+$ transitions, are not addressed here. The corresponding seven TDMs and four PDMs obtained by icMRCI+Q method with the aug-cc-pwCV5Z-DK basis set are presented in Fig. 3. The TDMs for the $A^2\Pi$ - $X^2\Sigma^+$ transition and the PDMs for the $X^2\Sigma^+$ and $A^2\Pi$ states are in quite good agreement with those computed by Kulik, Steeves & Field (2009), Knowles & Werner (1988), and Yin et al. (2018). The TDMs for the $3^2\Pi$–$B^2\Sigma^+$ and $4^2\Pi$–$B^2\Sigma^+$ transitions are very similar as both $3^2\Pi$ and $4^2\Pi$ states have the same electron composition ($1\sigma^2 2\sigma^2 3\sigma^2 4\sigma^2 5\sigma^2 1\pi^2 2\pi^1$), differing only in the coupling of the angular momentum.

3.2 Radiative association cross sections and rate coefficients

3.2.1 Considering the collision of the ground-state C and N atoms

Radiative association cross sections for eight transition processes corresponding to the first dissociation limit are calculated utilizing the QM method that considers the contribution of the resonance, as shown in Fig. 4. The $X^2\Sigma^+ \to X^2\Sigma^+$ and $b^4\Pi \to a^4\Sigma^+$ transitions are dominant at the collision energy from 0.002 eV to 10 eV. For the

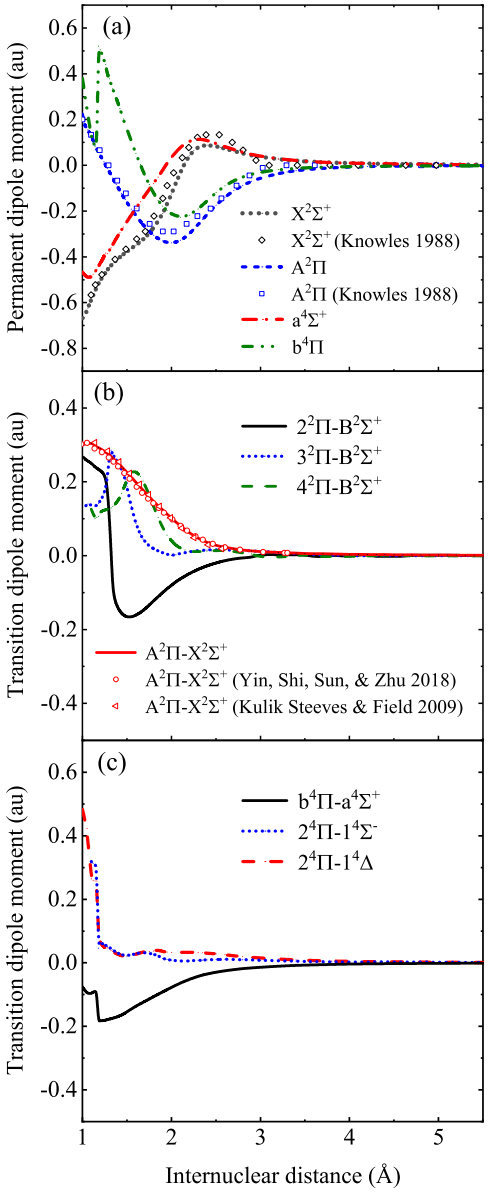

Figure 3. The results of CN calculated by the icMRCI+Q /aug-cc-pwCV5Z-DK method for (a) the PDMs of the $X^2\Sigma^+$, $A^2\Pi$, $a^4\Sigma^+$ and $b^4\Pi$ states, and the comparison of the PDMs for ^{2}X Σ^+ and $A^2\Pi$ electronic states with those computed by Knowles et al. (1988), (b) the TDMs of the $2^2\Pi$–$B^2\Sigma^+$, $3^2\Pi$–$B^2\Sigma^+$, $4^2\Pi$–$B\ ^2\Sigma^+$, and $A^2\Pi$–$X^2\Sigma^+$ transitions, and the comparison of the $A^2\Pi$–$X^2\Sigma^+$ transition with those computed by Yin et al. (2018) and Kulik et al. (2009), and (c) the TDMs of the $b^4\Pi$–$a^4\Sigma^+$, $2^4\Pi$–$1^4\Sigma^-$, and $2^4\Pi$–$1^4\Delta$ transitions.

collision energy lower than about 0.008 eV, the cross sections of the $b\ ^4\Pi \rightarrow a^4\Sigma^+$ transition are larger than those of the $A^2\Pi \rightarrow X^2\Sigma^+$ transition. The contribution of the $b^4\Pi \rightarrow a^4\Sigma^+$ transition cannot be ignored at the range for collision energy larger than 0.008 eV. Noted that the cross sections of the other six transitions are insignificant.

Rate coefficients are calculated by averaging the cross sections over a Maxwellian velocity distribution in the temperature range of 10–20 000 K. The results for eight radiative association processes and the total rate coefficients are shown in Fig. 5. The rate coefficients of the $A^2\Pi \rightarrow X^2\Sigma^+$ transition are in good agreement with those computed by Antipov (2009). Both the $b\ ^4\Pi \rightarrow a^4\Sigma^+$ and $A^2\Pi \rightarrow X^2\Sigma^+$ transitions are significant during the entire temperature range. The $b^4\Pi \rightarrow a^4\Sigma^+$ transition dominates the total rate coefficients for the temperatures below about 50 K, while the $A^2\Pi \rightarrow X^2\Sigma^+$ transition is dominant when the temperature is larger than 50 K. The contribution of other six transition processes is insignificant to the total rate coefficients.

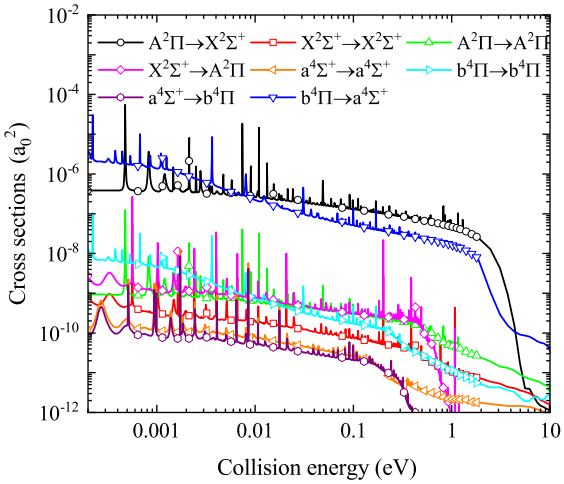

Figure 4. Radiative association cross sections of the CN molecule as the function of collision energy for the $A^2\Pi \rightarrow X^2\Sigma^+$, $X^2\Sigma^+ \rightarrow A^2\Pi$, $A^2\Pi \rightarrow A^2\Pi$, $X^2\Sigma^+ \rightarrow X^2\Sigma^+$, $b^4\Pi \rightarrow a^4\Sigma^+$, $a^4\Sigma^+ \rightarrow b^4\Pi$, $b^4\Pi \rightarrow b^4\Pi$, and $a^4\Sigma^+ \rightarrow a^4\Sigma^+$ transition systems.

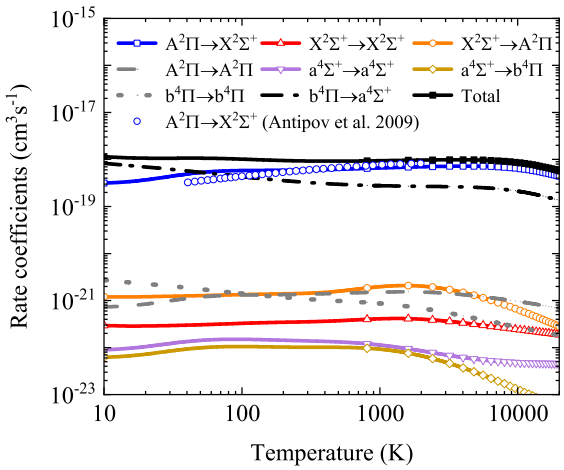

Figure 5. The total rate coefficients and the rate coefficients of the calculated eight transition processes for the radiative association of the CN molecule. The comparison of the $A^2\Pi \rightarrow X^2\Sigma^+$ transition with that from Antipov et al. (2009) is presented as well.

The total rate coefficients for the radiative association of CN can be approximated using the three-parameter Arrhenius–Kooij function (Laidler 1996), which is expressed as

$$k(T) = A\left(\frac{T}{300}\right)^{\alpha} \mathrm{e}^{-\beta/T}. \quad (21)$$

where A, α, and β are fitting parameters. The fitting parameters are summarized in Table 2. The fitted rate coefficients deviate less than one percent from our computed ones.

Table 2. Fitting parameters for the total rate coefficients considering the association of the ground C (^3P_g) and N (^4S_u) atoms.

T (K)	A (cm^3 s^{-1})	α	β (K)
10–200	9.61246×10^{-19}	−0.02459	−1.38223
200–2000	8.35012×10^{-19}	0.07297	−31.47702
2000–4000	1.16128×10^{-18}	−0.04537	185.53633
4000–10 000	7.39996×10^{-18}	−0.5417	2480.71392
10 000–20 000	1.22611×10^{-16}	−1.17511	8414.82611

3.2.2 Considering the collision of C and N atoms in their ground and excited states

When considering the collision of C and N atoms in their ground and excited states corresponding to three different asymptotic energies, the population factors $\tilde{P}_n$ are used to account for the thermal population of these asymptotes, as done by Antipov et al. (2011). $\tilde{P}_n$ can be given by

$$\tilde{P}_n = \frac{g_n e^{-\frac{\varepsilon_n}{k_B T}}}{\sum g_n e^{-\frac{\varepsilon_n}{k_B T}}}, \tag{22}$$

where g_n and ε_n are the degeneracy and the energy of the nth asymptote, respectively. k_B is the Boltzmann constant. The population factors in $g_{\Lambda'}$ in equation (16) should be substituted by $P_{\Lambda'}$ as

$$P_{\Lambda'} = \tilde{P}_n \times g_{\Lambda'}. \tag{23}$$

Selecting the first asymptote as the zero level, ε_1 is zero, ε_2 is 10162.582 cm^{-1}, and ε_3 is 19760.575 cm^{-1}. The $\tilde{P}_1$ for the reactions (1)–(8), $\tilde{P}_2$ for the reaction (9), and $\tilde{P}_3$ for the reactions (10)–(12) are given by

$$\tilde{P}_1 = \frac{36}{36 + 20 \times e^{-\frac{\varepsilon_2}{k_B T}} + 90 \times e^{-\frac{\varepsilon_3}{k_B T}}}, \tag{24}$$

$$\tilde{P}_2 = \frac{20 \times e^{-\frac{\varepsilon_2}{k_B T}}}{36 + 20 \times e^{-\frac{\varepsilon_2}{k_B T}} + 90 \times e^{-\frac{\varepsilon_3}{k_B T}}}, \tag{25}$$

$$\tilde{P}_3 = \frac{90 \times e^{-\frac{\varepsilon_3}{k_B T}}}{36 + 20 \times e^{-\frac{\varepsilon_2}{k_B T}} + 90 \times e^{-\frac{\varepsilon_3}{k_B T}}}. \tag{26}$$

The temperature-dependent part of the population $\tilde{P}_n$ is not included for the computation of radiation association cross sections. The cross sections of all transition processes including the association of N (^4S_u) and C (^1D_g) atoms, and C (^3P_g) and N (^2D_u) atoms are shown in Fig. 6. The $2^4\Pi \rightarrow 1^4\Sigma^-$ transition process exhibits a sharply variation at the collision energy of about 1.68 eV as the $2^4\Pi$ electronic state exhibits a potential barrier at R = 1.7 Å. The cross sections for the $2^2\Pi \rightarrow B^2\Sigma^+$, $3^2\Pi \rightarrow B^2\Sigma^+$ and $4^2\Pi \rightarrow B^2\Sigma^+$ transitions are dominant at collision energies larger than about 0.1 eV because of the deep potential well of the $B^2\Sigma^+$ state. The $2^2\Pi \rightarrow B^2\Sigma^+$ transition contributes most due to its larger TDMs.

The rate coefficients for the 12 transition processes and the total rate coefficients are calculated at the temperature range of 10–20 000 K and are shown in Fig. 7. The temperature-dependent part of the population factor $\tilde{P}_n$ is included in the computation of rate coefficients. The results show that rate coefficients of the transitions belonging to the first dissociation asymptote show a downward trend with the increasing temperature since the population factor of the first dissociation asymptote becomes smaller as temperature increases. As expected from the cross sections, the contribution of rate coefficients for the $2^2\Pi \rightarrow B^2\Sigma^+$, $3^2\Pi \rightarrow B^2\Sigma^+$, and $4^2\Pi \rightarrow B^2\Sigma^+$ transitions

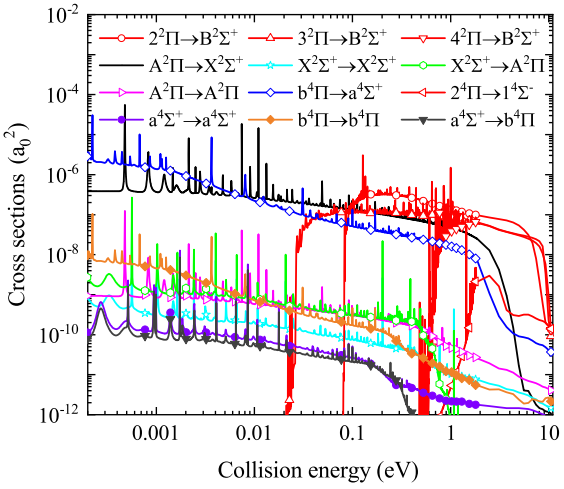

Figure 6. Radiative association cross sections of the CN molecule as the function of collision energy for the $A^2\Pi \rightarrow X^2\Sigma^+$, $X^2\Sigma^+ \rightarrow A^2\Pi$, $A^2\Pi \rightarrow A^2\Pi$, $X^2\Sigma^+ \rightarrow X^2\Sigma^+$, $b^4\Pi \rightarrow a^4\Sigma^+$, $a^4\Sigma^+ \rightarrow b^4\Pi$, $b^4\Pi \rightarrow b^4\Pi$, $a^4\Sigma^+ \rightarrow a^4\Sigma^+$, $2^4\Pi \rightarrow 1^4\Sigma^-$, $2^2\Pi \rightarrow B^2\Sigma^+$, $3^2\Pi \rightarrow B^2\Sigma^+$, and $4^2\Pi \rightarrow B^2\Sigma^+$ transition systems.

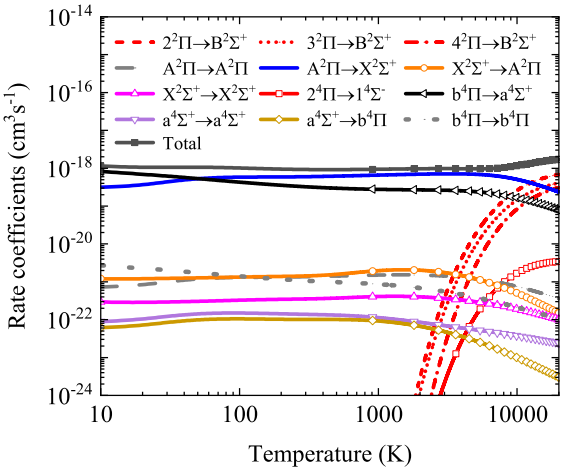

Figure 7. The total rate coefficients and the rate coefficients of the calculated twelve transition processes for the radiative association of the CN molecule.

Table 3. Fitting parameters for the total rate coefficients considering the association of C (^3P_g) and N (^4S_u), C (^1D_g) and N (^4S_u), and C (^3P_g) and N (^2D_u) atoms.

T (K)	A (cm^3 s$^-1$)	α	β (K)
10–200	9.61248×10^{-19}	−0.02459	−1.38224
200–2000	8.35422×10^{-19}	0.07266	−31.33237
2000–3000	1.21674×10^{-18}	−0.06387	208.59893
3000–5000	1.13657×10^{-18}	−0.04738	113.3207
5000–7000	5.47933×10^{-20}	0.74702	−3873.73116
7000–10 000	4.3497×10^{-21}	1.36979	−7879.36832
10 000–20 000	1.48364×10^{-18}	0.11205	6441.8216

to the total rate coefficients cannot be ignored at temperatures larger than about 10 000 K. The total rate coefficients for considering twelve transition processes are fitted using equation (21). The fitting parameters are summarized in Table 3.

4 CONCLUSION

In this work, we have computed the PECs, TDMs, and PDMs for CN at the icMRCI+Q/aug-cc-pwCV5Z-DK level of theory in which eleven electronic states are considered. Radiative association cross sections have been then computed by the QM method. The rate coefficients are obtained for the temperatures of 10–20 000 K. The cross sections for the $A^2\Pi \rightarrow X^2\Sigma^+$, $b^4\Pi \rightarrow a^4\Sigma^+$, $2^2\Pi \rightarrow B^2\Sigma^+$, $3^2\Pi \rightarrow B^2\Sigma^+$, and $4^2\Pi \rightarrow B^2\Sigma^+$ transition processes are significant. The contribution of the $A^2\Pi \rightarrow X^2\Sigma^+$ and $b^4\Pi \rightarrow a^4\Sigma^+$ transitions to the total rate coefficients are essential over the entire temperature range. The $b^4\Pi \rightarrow a^4\Sigma^+$ transition dominates the total rate coefficients at temperatures below about 50 K. For temperatures from about 50 to 20 000 K, the $A^2\Pi \rightarrow X^2\Sigma^+$ transition is dominant. After considering the effect of the radiative association involving the excited atoms the contribution of the $2^2\Pi \rightarrow B^2\Sigma^+$, $3^2\Pi \rightarrow B^2\Sigma^+$, and $4^2\Pi \rightarrow B^2\Sigma^+$ transitions to the total rate coefficients cannot be ignored for temperatures larger than about 10 000 K. The calculated cross sections and rate coefficients are significant to study the CN chemical evolution in the interstellar space.

ACKNOWLEDGEMENTS

This work is sponsored by National Natural Science Foundation of China (52106098), Natural Science Foundation of Shandong Province (ZR2021QE021), China Postdoctoral Science Foundation (2021M701977), Postdoctoral Innovation Project of Shandong Province, and Postdoctoral Applied Research Project of Qingdao City. The scientific calculations in this paper have been done on the HPC Cloud Platform of Shandong University.

CONFLICT OF INTEREST

There are no conflicts to declare.

DATA AVAILABILITY STATEMENT

Full data are available. The supplemental materials include the eleven PECs, seven TDMs, and two PDMs for CN (corresponding to Figs 2 and 3), as well as the cross sections and rate coefficients of the radiative association processes (corresponding to Figs 5–7). The cross sections and rate coefficients can also be obtained online at https://dr-zhi-qin.github.io/personal/Database.html.

REFERENCES

Antipov S. V., Sjölander T., Nyman G., Gustafsson M., 2009, J. Chem. Phys., 131, 74302
Antipov S. V., Gustafsson M., Nyman G., 2011, J. Chem. Phys., 135, 184302
Bachiller R., Fuente A., Bujarrabal V., Colomer F., Loup C., Omont A., de Jong T., 1997, A&A, 319, 235
Bai T., Qin Z., Liu L., 2021, MNRAS, 500, 2496
Bai T., Qin Z., Liu L., 2022, MNRAS, 510, 1649
Balucani N. et al., 2010, Faraday Discuss., 147, 189
Black J. H., van Dishoeck E. F., 1988, ApJ, 331, 986
Combi M. R., 1980, ApJ, 241, 830
Crawford I. A., 1995, MNRAS, 277, 458
Dalgarno A., Du M. L., You J. H., 1990, ApJ, 349, 675
Durić N., Erman P., Larsson M., 1978, Phys. Scr., 18, 39
Feldman P. D., Brune W. H., 1976, ApJ, 209, L45
Gerin M., Combes F., Encrenaz P., Linke R., Destombes J. L., Demuynck C., 1984, A&A, 136, L17
Gerlich D., Horning S., 1992, Chem. Rev., 92, 1509
Greaves J. S., Church S. E., 1996, MNRAS, 283, 1179
Gustafsson M., 2013, J. Chem. Phys., 138, 74308
Gustafsson M., Forrey R. C., 2019, J. Chem. Phys., 150, 224301
Hansson A., Watson J. K. G., 2005, J. Mol. Spectrosc., 233, 169
Huber K. P., Herzberg G., 1979, Molecular Spectra and Molecular Structure. Van Nostrand Reinhold Company, New York
Johnson B. R., 1977, J. Chem. Phys., 67, 4086
Johnson B. R., 1978, J. Chem. Phys., 69, 4678
Johnson J. R., Fink U., Larsson H. P., 1983, ApJ, 270, 769
Klemperer W., 1971, Highlights Astron., 2, 421
Knowles P. J., Werner H. J., 1985, Chem. Phys. Lett., 115, 259
Knowles P. J., Werner H. J., 1988, Chem. Phys. Lett., 145, 514
Knowles P. J., Werner H. J., 1992, Theor. Chim. Acta, 84, 95
Knowles P. J., Werner H. J., Hay P. J., Cartwright D. C., 1988, J. Chem. Phys., 89, 7334
Kramida A., Ralchenko Y., Reader J., Team NIST ASD, 2021, NIST Atomic Spectra Database (version 5.9). National Institute of Standards and Technology, Gaithersburg, MD, available at: https://physics.nist.gov/asd
Kulik H. J., Steeves A. H., Field R. W., 2009, J. Mol. Spectrosc., 258, 6
Laidler K., 1996, Pure Appl. Chem., 68, 149
Lambert D. L., 1968, MNRAS, 138, 143
Lambert D. L., 1978, MNRAS, 182, 249
Lambert D. L., Brown J. A., Hinkle K. H., Johnson H. R., 1984, ApJ, 284, 223
Lambert D. L., Sheffer Y., Crane P., 1990, ApJ, 359, L19
Lavendy H., Robbe J. M., Gandara G., 1987, J. Phys. B, 20, 3067
Magnasco V., Ficari G., Battezzati M., 1977, J. Chem. Phys., 66, 3742
Meyer D. M., Jura M., 1985, ApJ, 297, 119
Morton D. C., 1975, ApJ, 197, 85
Nyman G., Gustafsson M., Antipov S. V., 2015, Int. Rev. Phys. Chem., 34, 385
Prasad C. V. V., Bernath P. F., 1992, J. Mol. Spectrosc., 56, 327
Qin Z., Bai T., Liu L., 2021, MNRAS, 507, 2930
Ram R. S., Davis S. P., Wallace L., Engleman R., Appadoo D. R. T., Bernath P. F., 2006, J. Mol. Spectrosc., 237, 225
Rosati R. E., Pappas D., Johnsen R., Golde M. F., 2007, J. Chem. Phys., 126, 154303
Shamasundar K. R., Knizia G., Werner H., 2011, J. Chem. Phys., 135, 54101
Shi D., Li W., Sun J., Zhu Z., 2011, J. Quant. Spectrosc. Radiat. Transf., 112, 2335
Singh P. D., Andreazza C. M., 2000, ApJ, 537, 261
Singh P. D., Sanzovo G. C., Borin A. C., Ornellas F. R., 1999, MNRAS, 303, 235
Smith D., 1993, Int. J. Mass Spectrom. Ion Process., 129, 1
Sneden C., Lambert D. L., 1982, ApJ, 259, 381
Szabó P., Góger S., Gustafsson M., 2021, Front. Astron. Space Sci., 8, 704953
Turner B. E., Gammon R. H., 1975, ApJ, 198, 71
Watson J. K. G., 2008, J. Mol. Spectrosc, 252, 5
Werner H. J., Knowles P. J., 1985, J. Chem. Phys., 82, 5053
Werner H. J., Knowles P. J., 1988, J. Chem. Phys., 89, 5803
Werner H. J.et al. 2015, Molpro 2015 edition, A Package of Ab Initio Programs. See http://www.molpro.net
Werner H. J. et al., 2020, J. Chem. Phys., 152, 144107
Wootten A., Lichten S. M., Sahai R., Wannier P. G., 1982, ApJ, 257, 151
Yin Y., Shi D., Sun J., Zhu Z., 2018, ApJS, 235, 25

SUPPORTING INFORMATION

Supplementary data are available at *MNRAS* online.

Supplemental materials.zip

Please note: Oxford University Press is not responsible for the content or functionality of any supporting materials supplied by the authors. Any queries (other than missing material) should be directed to the corresponding author for the article.

This paper has been typeset from a TEX/LATEX file prepared by the author.